ISSN 0965-5425, Computational Mathematics and Mathematical Physics, 2016, Vol. 56, No. 1, pp. 161–172. © Pleiades Publishing, Ltd., 2016.
Original Russian Text © K.K. Abgaryan, D.L. Reviznikov, 2016, published in Zhurnal Vychislitel'noi Matematiki i Matematicheskoi Fiziki, 2016, Vol. 56, No. 1, pp. 155–166.

Numerical Simulation of the Distribution of Charge Carrier in Nanosized Semiconductor Heterostructures with Account for Polarization Effects

K. K. Abgaryan[a] and D. L. Reviznikov[b]

[a] *Dorodnicyn Computing Center, Russian Academy of Sciences, ul. Vavilova 40, Moscow, 119333 Russia*
[b] *Moscow Aviation Institute (National Research University), Volokolamskoe shosse 4, Moscow, 125993 Russia*
e-mail: kristal83@mail.ru

Received March 12, 2015; in final form, June 4, 2015

Abstract—A three-level scheme for modeling nanosized semiconductor heterostructures with account for spontaneous and piezoelectric polarization effects is presented. The scheme combines quantum-mechanical calculations at the atomic level for obtaining the charge density on heterointerfaces, calculation of the distribution of carriers in the heterostructure based on the solution to the Schrödinger and Poisson equations, and the calculation of electron mobility in the two-dimensional electron gas with account for various scattering mechanisms. To speed up the computations of electron density in the heterostructure, the approach based on the approximation of the nonlinear dependence of the electron density on the potential in combination with the linearization of the Poisson equation is used. The efficiency of this approach in problems of the class in question is demonstrated.

Keywords: Numerical simulation, semiconductor heterostructures, Schrödinger and Poisson equations, electron density, mobility of charge carriers.

DOI: 10.1134/S0965542516010048

INTRODUCTION

The modern trend in the development of high-frequency semiconductor engineering is the aspiration to miniaturization, maximization of the concentration of charge carriers, and maximization their mobility. To this end, multilayer nanosized heterostructures are used in which the motion of charge carriers in one or more directions is restricted due to potential barriers (see [1]). The main factors affecting the localized carrier (two-dimensional electron gas) transport channels in the vicinity of the heterointerface are the concentration of doping carriers in the barrier layer and the presence of a surface charge on the heterointerface. The surface charge is characteristic of wurtzite structures—it is caused by spontaneous and piezoelectric polarization (see [2]).

In the Computing Center of the Russian Academy of Sciences, the following procedure for multiscale simulation of semiconductor structures has been implemented (see [3]). Three characteristic scale levels are distinguished. At the atomic level, the system is described using crystallographic information (see [4]) and a quantum mechanical model based on the electron density functional theory [5, 6]. The results are passed to the nanoscale model, where they are used to calculate the distribution of charge carriers in the heterostructure. At this level, the mathematical model is a system of the Schrödinger and Poisson equations (see [7]). The use of the concept of effective electron mass allows us to avoid the detailed consideration of interactions of electrons with the nuclear frame and thus change from the atomic scale to real nanosized heterostructure scale. Of major interest is the distribution of charge carrier density across the multilayer structure and the detection of a localized high-concentration band (electron gas). For the heterosystems in which the quantum restriction is achieved by doping the barrier layer with impurities, the Poisson equation includes a distributed source. In wurtzite structures, there is spontaneous and piezoelectric polarization as a result of which the charge is concentrated in the interlayer interface. This results in the occurrence of a strong localized source; therefore, the solution must have a high resolution. The data about the wave functions and the distribution of charge carrier density across the multilayer structure obtained by solving the Schrödinger and Poisson adjoint equations are fed to the next level model, where the mobility of carries in the longitudinal direction is calculated. In this calculation, a wide range of scat-

tering mechanisms—scattering by optical and acoustic phonons, by the roughnesses of the heterointerface, by charged centers and dislocations, and piezoelectric scattering—are taken into account (see [3]).

In this paper we focus on numerical simulation on the nanoscale level. At this level, the local computational procedures used to solve the Schrödinger and Poisson equations are combined in a unified iteration process aimed at making the solutions self-consistent. A key point is a strong interrelation of equations, which is characteristic for this class of problems; hence, the convergence problem of global iterations arises. This problem is especially significant in the case of wurtzite structures, where a strong localized charge source appears on heterointerfaces.

MATHEMATICAL MODEL

A typical scheme of a nanosized semiconductor heterostructure is shown in Fig. 1 (borrowed from [8]).

This heterostructure was grown in the Institute of Semiconductor Physics of the Siberian Branch of the Russian Academy of Sciences based on gallium nitride and triple solutions (see [8]). The presence of layers made of semiconductors with different width of the forbidden gap in combination with polarization effects ensures the creation of a quantum well for electrons of a width of several nanometers in the neighborhood of the heterointerface in the layer with the lower width of the forbidden gap (GaN). The motion of electrons in the direction perpendicular to the heterointerface is bounded, and the energy levels are quantized. In these levels, the electron can freely move in the plane of the heterointerface. Two-dimensional electron gas is formed (the region where the two-dimensional electron gas is formed is shown by dots in Fig. 1).

The mathematical model describing the distribution of electrons in such structures is a system of the Schrödinger and Poisson equations (see [7, 9]). Note that the motion of charge carriers in semiconductor devices can be restricted not only in one direction (two-dimensional electron gas) but also in two (quantum wire) and three (quantum point) directions (see [1]). This is usually achieved by applying voltage in the corresponding bands. In the general case, the problem of simulating heterostructures is stated in three-dimensions. The mathematical model is as follows:

$$-\frac{\hbar^2}{2}\nabla\cdot\left(\frac{1}{m^*}\nabla\psi\right)+(-e\varphi+\Delta E_c)\psi=E\psi, \tag{1}$$

$$\nabla\cdot(\varepsilon\nabla\varphi)=-e(N_D(z)-N_A(z)-n(\mathbf{r}))+\sum_l \sigma_l\delta(z-z_l), \tag{2}$$

$$n(\mathbf{r})=\sum_i(\psi_i(\mathbf{r}))^2 n_i, \tag{3}$$

$$n_i=k_BT\frac{m^*}{\pi\hbar^2}\ln\left(1+\exp\left(\frac{E_F-E_i}{k_BT}\right)\right). \tag{4}$$

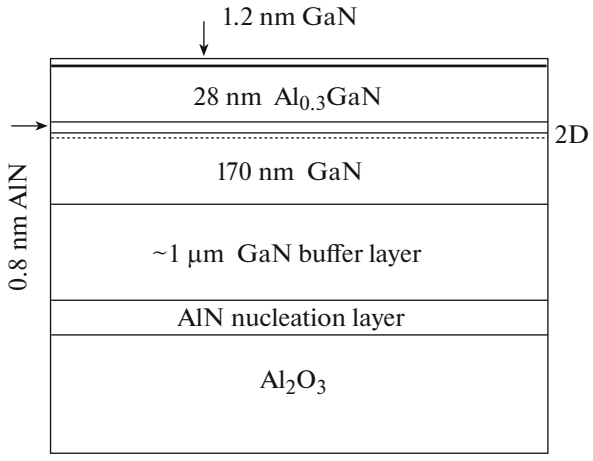

Fig. 1. Multilayer semiconductor heterostructure (see [8]).

Here E_i and $\psi_i(\mathbf{r})$ are energy levels an corresponding wave functions, $n(\mathbf{r})$ is the electron density, $\hbar$ is Planck's constant, $e$is the electron charge, m^* is the effective electron mass, E_F is the position of the Fermi level, $\varphi(\mathbf{r})$ is the electrostatic potential, N_d, N_A are the concentrations of the donor and acceptor impurities, σ_l are the densities of charges on the interfaces, δ is the delta function, z_l are the positions of the interfaces, ε is the dielectric constant of the material, ΔE_c is the shift of the conduction band of the material, k_B is Boltzmann's constant, and T is the temperature. Model (1)–(4) takes into account the fact that m^*, ε, and ΔE_c may vary from level to level. However, the temperature in the heterostructure remains constant.

In the notation of Eqs. (1)–(4), the transverse direction (the coordinate z) is distinguished, which reflects the layer-by-layer growth of the structure and the dependence of certain characteristics only on this coordinate.

Problem (1)–(4) is typically solved in a rectangular domain Ω (an example of such a domain is shown in Fig. 1), which is typical for many semiconductor devices. The conditions on the boundary Γ of Ω must reflect the heterostructure operation. Typically, Ω is much larger than the domain in which the quantum restriction is realized; therefore, it is reasonable to state the uniform Dirichlet boundary condition for the wave function: $\psi|_\Gamma = 0$. Depending on the heterostructure operational conditions, the conditions for the electrostatic potential on different parts of the boundary can be specified as the values of the applied voltage (Dirichlet boundary conditions $\varphi|_\Gamma = \varphi_g$), or as the values of the electric field strength (the Neumann boundary conditions $\left.\frac{\partial\varphi}{\partial\eta}\right|_\Gamma = f_g$, where $\frac{\partial\varphi}{\partial\eta}$ is the normal derivative). The first type of boundary conditions is typical for problems in which the quantum restrictions are reached due to an external electric field (quantum wires in the two-dimensional case and quantum points in the three-dimensional case) and in the contact regions between the semiconductor and metals. The second type is often used on the boundary at the substrate side, where the electric field strength is zero (the uniform Neumann boundary condition.

The solution to the eigenvalue problem (1) (the Schrödinger equation) depends on the electrostatic potential φ, the distribution of which in the structure $\varphi(\mathbf{r})$ is determined by the Poisson equation (2). The right-hand side of the Poisson equation includes the electron density $n(\mathbf{r})$, which, in turn, is determined by the energy levels E_i and the wave functions $\psi_i(\mathbf{r})$ according to the Fermi–Dirac statistics (3), (4). Therefore, the problem is clearly of the adjoint type.

The self-consistent solution to this systems gives the desired energy levels E_i and the corresponding wave functions $\psi_i(\mathbf{r})$, the profile of the potential well $V(\mathbf{r})$, and the distribution of electron density in the heterostructure $n(\mathbf{r})$.

Let us briefly discuss how the main factors affecting the emergence of localized channels of charge carrier transport in the vicinity of the heterointerface are represented in the mathematical model.

The expression for the electron potential energy in Eq. (1) $V = -e\varphi + \Delta E_c$ includes the shift ΔE_c of the conduction band in the semiconductor material that causes the creation of a potential barrier, which confines electrons to the quantum well.

For semiconductors with the sphalerite crystal structure, the most important factor is the concentration N_D of donors in the barrier layer; this concentration appears on the right-hand side of the Poisson equation. For semiconductors with the wurtzite crystal structure, the major role is played by polarization effects and related surface charges on heterointerfaces. This factor is represented in the mathematical model by the term $\sum_l \sigma_l \delta(z - z_l)$ in the Poisson equation. In this case, the two-dimensional electron gas appears even without introducing donors into the barrier layer. The spontaneous and piezoelectric polarization effects are described by quantum-mechanical models at the atomic level, which makes it possible to calculate the densities of the surface charge on the interfaces (see [10]).

It is clear that the distribution of electron density in the multilayer heterostructure is affected by the width and position of layers, as well as by other parameters of the mathematical model.

Many problems concerning the calculation and optimization of multilayer semiconductor structures are solved in the spatially one-dimensional statement, which allows one to determine the basic characteristics of the two-dimensional electron gas. In this case, the mathematical model is as follows.

$$-\frac{\hbar^2}{2}\frac{d}{dz}\left(\frac{1}{m^*(z)}\frac{d\psi}{dz}\right)+V(z)\psi(z)=E\psi(z),$$

$$\frac{d}{dz}\left(\varepsilon(z)\frac{d\varphi}{dz}\right)=-e(N_D(z)-N_A(z)-n(z))+\sum_l \sigma_l\delta(z-z_l),$$

$$V(z)=-e\varphi(z)+\Delta E_c(z),$$

$$n(z)=\sum_i(\psi_i(z))^2 n_i(z),$$

$$n_i(z)=k_BT\frac{m^*(z)}{\pi\hbar^2}\ln\left(1+\exp\left(\frac{E_F-E_i}{k_BT}\right)\right).$$

Note that difficulties due to the convergence of global iterations for obtaining a self-consistent solution to the Schrödinger and Poisson equations clearly manifest themselves when the one-dimensional problem is solved. For this reason, the analysis in this paper is based on the one-dimensional model.

Consider the statement of the boundary conditions in more detail.

On the boundaries of the system ($z=0$, $z=L$, where L is the total thickness of the multilayer structure) the wave functions must vanish:

$$\psi(0)=0,\quad \psi(L)=0.$$

On the left boundary $z=0$, a potential barrier φ_b, which is formed in the contact semiconductor–metal layer (Schottky barrier) is typically specified. In addition, the shift φ_s due to the applied voltage may be specified. The behavior of the potential on the right boundary $z=L$ is determined by the position of the conduction band of the corresponding material relative to the Fermi level. In most cases, a natural condition in this case is the absence of the electric field. Thus, the boundary conditions for the Poisson equation are

$$\varphi(0)=\varphi_b+\varphi_s,\quad \varphi'(L)=0.$$

COMPUTATIONAL ALGORITHMS

It has already been mentioned above that the equations in the problem are coupled; therefore, the solutions to the Schrödinger and Poisson equations must be iteratively made consistent. To this end, the local computational procedures used for solving these equations are joined into a global iterative loop. The computation process can be schematically represented as follows.

After executing an iteration step, we have the distribution $n^{(k)}(\mathbf{r})$ of the electron density in the system.

Using this information, we solve the Poisson equation

$$\nabla\cdot(\varepsilon\nabla\varphi^{(k+1)})=-e(N_D-N_A-n^{(k)})+\sum_l\sigma_l\delta(z-z_l).$$

The resulting distribution $\varphi^{(k+1)}$ of the potential in the system is used to solve the Schrödinger equation

$$-\frac{\hbar^2}{2}\nabla\cdot\left(\frac{1}{m^*}\nabla\psi^{(k+1)}\right)+(-e\varphi^{(k+1)}+\Delta E_c)\psi^{(k+1)}=E^{(k+1)}\psi^{(k+1)}.$$

As a result, we obtain significant (i.e. those that make a contribution to the increase of carrier concentration) energy levels and the corresponding wave functions $E_i^{(k+1)}$, $\psi_i^{(k+1)}$.

Next, using the Fermi–Dirac statistics, the new distribution of electron density in the system is calculated by the formula

$$n^{(k+1)} = \sum_i \left(\psi_i^{(k+1)}\right)^2 k_B T \frac{m^*}{\pi\hbar^2} \ln\left(1 + \exp\left(\frac{E_F - E_i^{(k+1)}}{k_B T}\right)\right).$$

In the class of problems under consideration, the equations are tightly coupled, which gives rise to the convergence problem of successive approximations. To ensure the convergence, the lower relaxation

$$\bar{n}^{(k+1)} = \omega n^{(k+1)} + (1 - \omega) n^{(k)},$$

where $\bar{n}^{(k+1)}$ is the final distribution of electron density on this iteration, can be used.

Numerical experiments on a wide class of semiconductor heterostructures show that a very small relaxation parameter ω should be used (the typical value of ω is 0.025), which considerably affects the convergence rate of global iterations. In a number of problems, an algorithm with an adaptive relaxation parameter can be constructed; however, this approach is difficult to be made universal. Note that similar difficulties as applied to the simulation of sphalerite structures were reported in [11]. The situation is much more complicated when semiconductors of wurtzite structure with charges localized on heterostructures are considered.

In this paper we solve this class of problems using an approach based on the local approximation of the implicit dependence of the electron density on the potential (see [11]). This approach proved to be effective in the simulation of the charge distribution in sphalerite heterostructures (see [12, 13]). The following approximate formula for the electron density was obtained using perturbation theory:

$$n(\varphi) \approx \sum_i \psi_i^2 k_B T \frac{m^*}{\pi\hbar^2} \ln\left(1 + \exp\left(\frac{E_F - E_i + e(\varphi - \varphi^{(k)})}{k_B T}\right)\right); \tag{5}$$

here, $\varphi^{(k)}$ is the potential obtained at the preceding global iteration step.

Since formula (5) considerably improves the efficiency of computational algorithms, we outline its derivation here.

Consider the increment of the potential $\delta\varphi = \varphi - \varphi^{(k)}$. The corresponding increment of the electron density δn caused by the variation of the wave functions $\delta\psi_i$ and the energy levels δE_i is

$$\delta n = A\sum_i (\psi_i + \delta\psi_i)^2 \ln\left(1 + \exp\left(F_i - \frac{\delta E_i}{k_B T}\right)\right) - A\sum_i (\psi_i)^2 \ln(1 + \exp F_i),$$

where $A = k_B T \dfrac{m^*}{\pi\hbar^2}$ and $F_i = \dfrac{E_F - E_i}{k_B T}$.

In the linear approximation, δn can be written as

$$\delta n = -A\sum_i \psi_i^2 \frac{\delta E_i}{k_B T} \frac{\exp F_i}{1 + \exp F_i} + 2A\sum_i \psi_i \delta\psi_i \ln(1 + \exp F_i).$$

According to linear perturbation theory (see [14]), we have

$$\delta E_i = -e(\psi_i, \delta\varphi\psi_i), \quad \delta\psi_i = -e\sum_{j\neq i} \psi_j \frac{(\psi_j, \delta\varphi\psi_i)}{E_i - E_j},$$

where $(\psi_j, \delta\varphi\psi_i) = \int_\Omega \psi_j \delta\varphi\psi_i dv$.

Taking into account the symmetry of the second term with respect to the indices, the formula for the electron density takes the form

$$\delta n = Ae\sum_i \psi_i^2 \frac{(\psi_i, \delta\varphi\psi_i)}{k_B T} \frac{\exp F_i}{1+\exp F_i}$$
$$- Ae\sum_i \sum_{j\neq i} \psi_i\psi_j(\psi_j, \delta\varphi\psi_i)\frac{\ln(1+\exp F_i) - \ln(1+\exp F_j)}{E_i - E_j}$$
$$\approx \frac{Ae}{k_B T}\sum_i \psi_i^2(\psi_i, \delta\varphi\psi_i)\frac{\exp F_i}{1+\exp F_i} + \frac{Ae}{k_B T}\sum_i\sum_{j\neq i}\psi_i\psi_j(\psi_j, \delta\varphi\psi_i)\frac{\exp F_i}{1+\exp F_i}.$$

Due to the orthonormal property of the wave functions, we have $\sum_{j\neq i}\psi_j(\psi_j, \delta\varphi\psi_i) = \delta\varphi\psi_i - \psi_i(\psi_i, \delta\varphi\psi_i)$, which yields

$$\delta n = \frac{Ae}{k_B T}\sum_i \psi_i^2 \frac{\exp F_i}{1+\exp F_i}\delta\varphi.$$

This allows us to obtain the desired approximation of the dependence of the electron density on the potential

$$n(\varphi) \approx n^{(k)} + \delta n = A\sum_i \psi_i^2 \ln\left(1+\exp\left(\frac{E_F - E_i}{k_B T}\right)\right)$$
$$+ \frac{Ae}{k_B T}\sum_i \psi_i^2 \frac{\exp F_i}{1+\exp F_i}\delta\varphi \approx A\sum_i \psi_i^2 \ln\left(1+\exp\left(\frac{E_F - E_i + e\delta\varphi}{k_B T}\right)\right).$$

The use of this approach yields the modified Poisson equation with the explicit nonlinear term $n(\varphi)$:

$$\nabla\cdot(\varepsilon\nabla\varphi) = -e(N_D - N_A - n(\varphi)) + \sum_l \sigma_l\delta(z - z_l).$$

The modified Poisson equation can be solved using the Newton–Raphson approximation (see [15]):

$$\varphi = \varphi^{(p)} + \xi,$$
$$\nabla\cdot(\varepsilon\nabla\xi) = g\xi + q,$$
$$g = e\frac{\delta n}{\delta\varphi}(\varphi^{(p)}),$$
$$q = -\nabla\cdot(\varepsilon\nabla\varphi^{(p)}) + (-e(N_D - N_A - n(\varphi^{(p)})) + \sum_l \sigma_l\delta(z - z_l).$$

Here the superscript (p) indicates the function obtained at the preceding local iteration step.

In this paper, we solve the Schrödinger and Poisson equations using finite difference methods. The approximation of derivatives by central differences reduces the problem at each global iteration step to solving the eigenvalue problem for a symmetric sparse banded matrix (a discrete analog of the Schrödinger equation) and to solving simultaneous algebraic equations (a discrete analog of the Poisson equation). The size of the matrices can be large because the resolution for the thin layer containing the two-dimensional electron gas must be sufficiently high; moreover, computations are repeated many times in the iterative process. Therefore, the algorithms must be computationally efficient. The solution of the discrete analog of the Schrödinger equation is the most computationally costly part. For this reason, we must take into account the position of the significant energy levels. According to the Fermi–Dirac statistics, the contribution to the increase of carrier concentration in the two-dimensional electron gas is made by the electrons on low energy levels. Information about the lower boundary is obtained from the solution to the Poisson equation at the current global iteration: $E_i^{(k)} > \min V^{(k)}(\mathbf{r})$. The upper level can be estimated using (4). It is of primary importance that, due to the features of the Fermi–Dirac distribution, the number of electrons with the energy exceeding the Fermi level more than by $k_b T$ decreases practically exponentially. This localization makes it possible to use efficient techniques for finding eigenvalues in combination with inverse iterations for determining the grid wave functions.

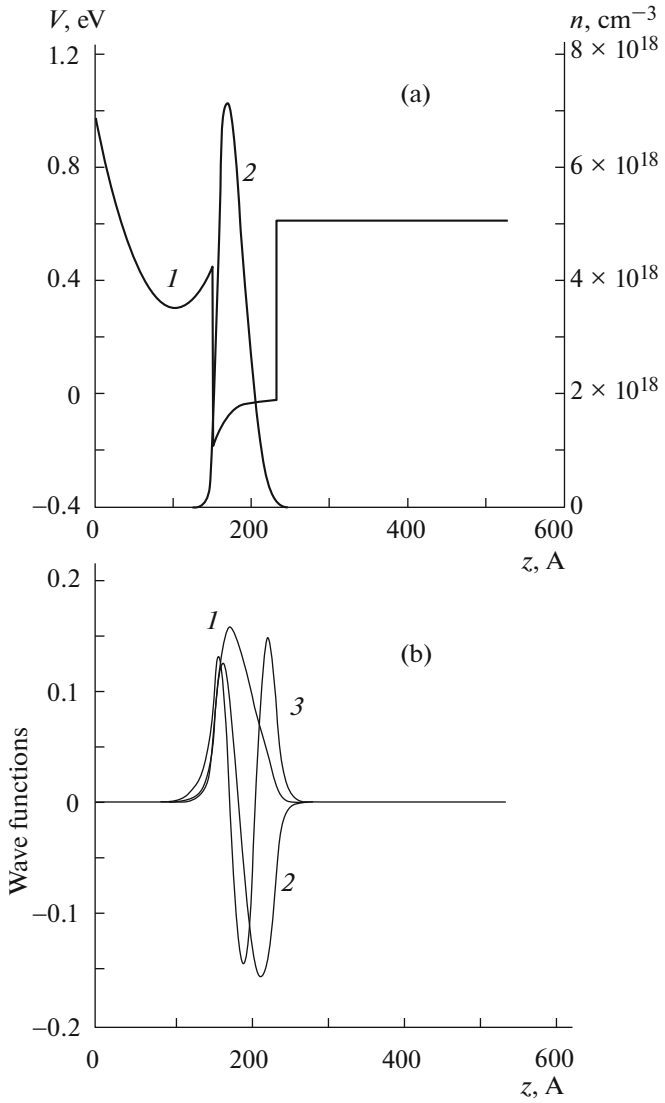

Fig. 2. (a) The distribution of the potential energy in the heterostructure depth (*1,* the left vertical axis) and electron density (*2,* the right vertical axis); (b) wave functions corresponding to the three lowest energy levels. Sphalerite crystal structure.

NUMERICAL EXPERIMENTS

First, we consider the case when the semiconductor materials have the sphalerite crystal structure. By way of example, consider the three-layer heterostructure $Al_{0.3}GaN/GaN/Al_{0.3}GaN$ (see [16]). The thickness of the layers is 15.2 nm for the $Al_{0.3}GaN$ barrier layer, 8 nm for the GaN layer, and 30 nm for the $Al_{0.3}GaN$ layer. The other data (see [16]) are as follows. The dielectric constants of the materials are $8.9\varepsilon_0$ for GaN and $8.5\varepsilon_0$ for $Al_{0.3}GaN$, where ε_0 is the permittivity of vacuum. The effective mass of the electron was assumed to be $0.228m_0$ for both materials (m_0 is the electron rest mass). The conduction band shift ΔE_c was assumed to be equal to 0.63 eV. The potential on the external surface of the heterostructure was found from the condition $-e\varphi(0) = 1$ eV (the energy was counted from the Fermi level).

We have already mentioned that in the case of a sphalerite crystal structure, the proper potential barriers are created by doping the barrier layer with a donor impurity. In the case under consideration, the volume concentration of impurity is 6×10^{18} cm^{-3}. Here and below in this section, we consider the one-dimensional problem. Figure 2 shows the distribution of the potential energy in the heterostructure depth (Fig. 2a, curve *1* with respect to the left vertical axis), the distribution of electron density (Fig. 2a, curve *2* with respect to the left vertical axis), and the wave functions (Fig. 2b, the curve indices correspond to increasing energy levels, beginning with the lowest one). In Fig. 2a, we clearly see a bend on the potential

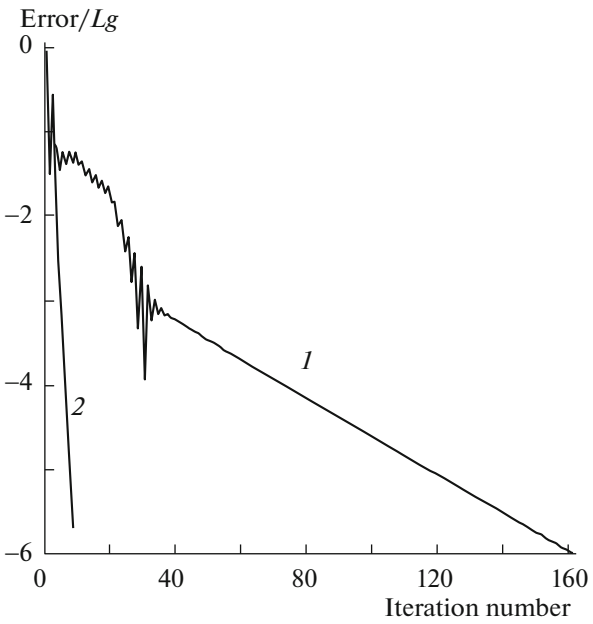

Fig. 3. Convergence of global iterations. Curve *1* corresponds to the successive lower relaxation method; *2* corresponds to the approximation of the nonlinear dependence of electron density on potential. Sphalerite crystal structure.

energy curve due to doping the barrier layer and a potential well in the GaN layer, which results in the formation of a localized band with a high electron density (two-dimensional electron gas). The total electron density in the two-dimensional electron gas is 3×10^{12} cm^{-2}. The results are in good agreement with the data presented in [16]. Figure 3 illustrates the convergence of global iterations for the structure in question. Here, curve *1* corresponds to the successive approximation method with lower relaxation; curve *2* corresponds to the approximation of the nonlinear dependence of electron density on potential (no lower relaxation is needed). The error was found as the difference between the lowest energy levels (the minimum eigenvalue for the Schrödinger equation) obtained at adjacent iterations. It is seen that the convergence rate is higher in the second case. In combination with the linearization of the Poisson equation, the proposed approach considerably reduces the computational cost. Note that the choice of difference between the lowest energy levels as the quantity characterizing the error was made in accordance with numerous numerical experiments, which show that the convergence with respect to the lowest energy levels ensures the convergence with respect to other possible criteria because the low energy electrons make the major contribution to the distribution of electron density, which ultimately affects the distribution of the electrostatic potential.

Now consider semiconductor materials with a wurtzite crystal structure. Consider the two-layer case $Al_{0.3}GaN/GaN$ (the thickness of the $Al_{0.3}GaN$ layer is 30 nm), which is thoroughly studied both experimentally and theoretically (see [2]). Here and in what follows, the initial data for computations were found using the approximation dependences (see [2])

$$\varepsilon_{AlGaN}(x) = (0.03x + 10.28)\varepsilon_0,$$

$$\Delta E_c(x) = 0.7(E_g(x) - E_g(0)), \quad E_g(x) = 6.13x + 3.42(1 - x),$$

$$-e\varphi_b = 1.3x + 0.84,$$

where x is the mole fraction of aluminum in the AlGaN alloy. The boundary value $\varphi(0) = \varphi_b$ for the potential was used.

Figure 4 shows the distributions of potential energy and electron density in the heterostructure depth and the wave functions. The curve enumeration is the same as in Fig. 2. The potential well profile and the formation of the two-dimensional electron gas are caused by the presence of a surface charge on the heterointerface. According to the ab initio quantum mechanical calculations (see [10]), the charge density is 1.34×10^{13} e C/cm^2. In this case, the total density of electrons in the two-dimensional electron gas is 1.14×10^{13} cm^{-2}, which is considerably higher than the similar density for sphalerite crystal materials. Fig-

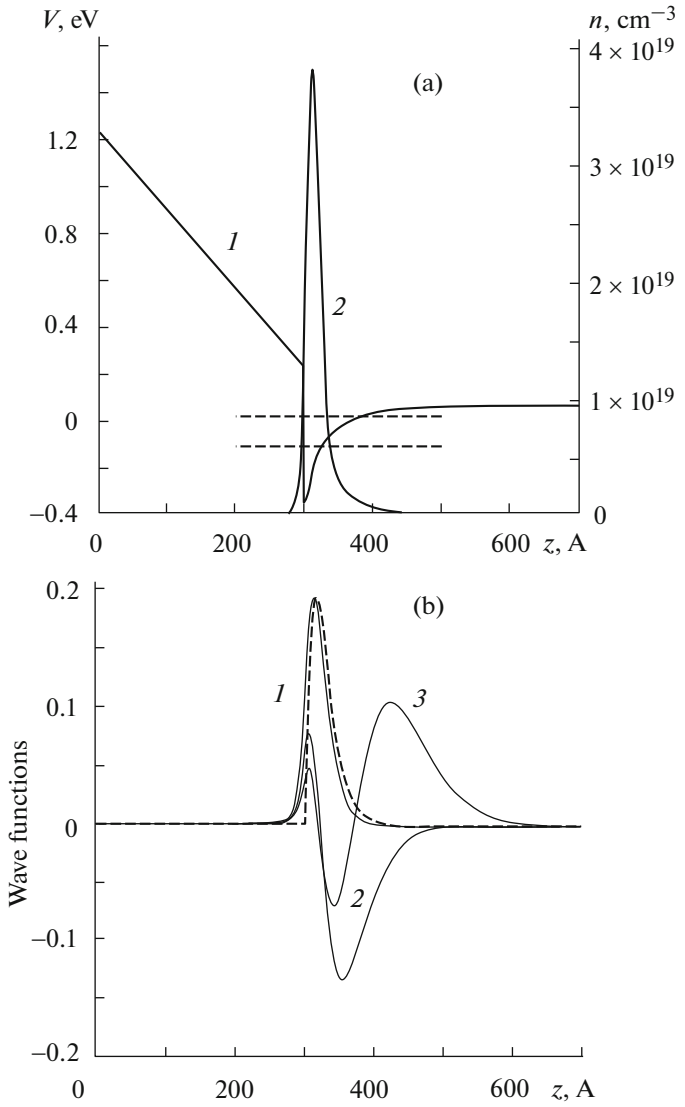

Fig. 4. (a) The distribution of the potential energy in the heterostructure depth (*1,* the left vertical axis) and electron density (*2,* the right vertical axis); (b) wave functions corresponding to the three lowest energy levels. Wurtzite crystal structure.

ure 5 illustrates the convergence of global iterations (the curve enumeration is the same as in Fig. 3). It is seen that the convergence of successive approximations is slower than in the case of the sphalerite crystal structure. The use of the approximation of the nonlinear dependence of electron density on the potential considerably accelerates the convergence of global iterations (almost by an order of magnitude in the case under consideration).

Figure 6 illustrates the dependences of the total density of electrons in the two-dimensional electron gas on the content of Al in the Al_xGaN layer. The solid curve represents the numerical solution and the x signs correspond to the approximation of experimental data (see [2]). It is seen that the numerical and experimental results are in good agreement.

In conclusion, we present in Fig. 7 numerical results for the multilayer structure shown in Fig. 1. The enumeration of curves is similar to that in Figs. 2a and 4a. In this structure, the GaN layer on the barrier layer surface prevents its oxidation. The role of the thin AlN layer can be seen in Fig. 7. In Figs. 4a and 7, we see a small difference in the distribution of the carrier concentration in the vicinity of the heterointerface. The interlayer AlN reduces the penetration of electrons into the barrier layer, which favors the higher

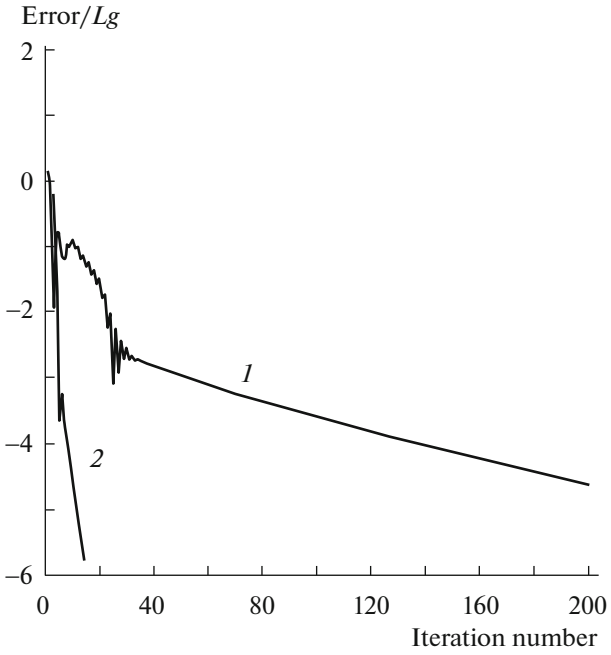

Fig. 5. Convergence of global iterations. Curve *1* corresponds to the successive lower relaxation method; *2* corresponds to the approximation of the nonlinear dependence of electron density on potential. Wurtzite crystal structure.

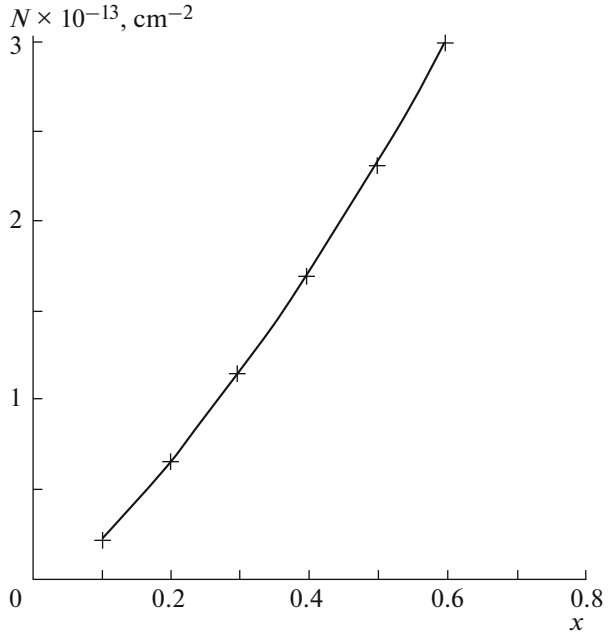

Fig. 6. The dependence of the total electron density in the two-dimensional electron gas on the Al concentration in the barrier layer. The solid curve represents the numerical solution and the x signs correspond to the approximation of experimental data (see [2]).

mobility of electrons in the two-dimensional electron gas. However, the difference in the total density of electrons is insignificant—about 1%.

Thus, the proposed numerical simulation methods and tools make it possibly to quickly analyze various multilayer nanosized heterostructures taking into account polarization effects. In combination with the simulation of mobility of charge carriers in such structures (see [3]), this creates a basis for solving a

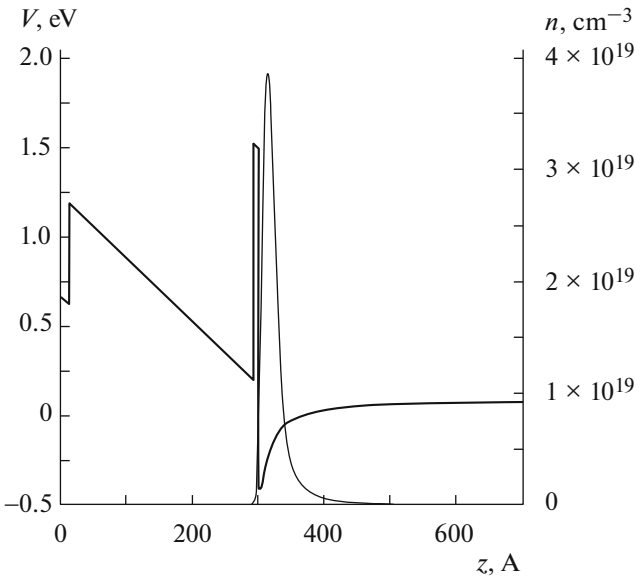

Fig. 7. The distribution of potential energy (*1*, left axis) and of the electron density (*2*, right axis) across the multilayer heterostructure (see [8]).

number of optimization problems in modern microwave electronics. Among these problems are the design of heterostructures that guarantee the maximum concentration of carriers and their maximum mobility (the maximum conductivity) and inverse problems of determining the characteristics of grown heterostructures based on experimental data concerning the concentration and mobility of carriers in the two-dimensional electron gas if these characteristics cannot be measured directly.

CONCLUSIONS

A three-layer scheme for simulating nanosized semiconductor heterostructures with account for spontaneous and piezoelectric polarization effects is described. It combines quantum mechanical calculations at the atomic level for calculating the charge density on heterointerfaces, the calculation of carrier distribution in the heterostructure based on solving the Schrödinger and Poisson equations, and the calculation of electron mobility in the two-dimensional electron gas with regard to various scattering mechanisms. To speed up the computations of electron density in the heterostructure, an approach based on the approximation of the nonlinear dependence of the electron density on potential in combination with the linearization of the Poisson equation is used. The efficiency of this approach for the problems in question is demonstrated. The proposed simulation methods and tools offer great capabilities for solving optimization problems that are important for microwave electronics.

ACKNOWLEDGMENTS

This work was supported by the Russian Science Foundation, project no. 14-11-00782.

REFERENCES

1. V. E. Borisenko, A. I. Vorob'eva, and E. A. Utkina, *Nanoelectronics* (Binom. Moscow, 2009) [in Russian].
2. O. Ambacher, J. Majewski, C. Miskys, A. Link, M. Hermann, M. Eickhoff, M. Stutzmann, F. Bernardini, V. Fiorentini, V. Tilak, B. Schaff, and L. F. Eastman, "Pyroelectric properties of Al(In)GaN/GaN hetero- and quantum well structures," J. Phys.: Condens. Matter, **14**, 3399–3434 (2002).
3. K. Abgaryan, I. Mutigullin, and D. Reviznikov, "Computational model of 2DEG mobility in the AlGaN/GaN heterostructures," Phys. Status Solidi, **C12**, 407–411 (2015).
4. K. K. Abgaryan and V. P. Khachaturov, "Computer simulation of stable structures in crystal substances," Comput. Math. Math. Phys. **49**, C. 1449–1462 (2009).
5. W. Kohn and L. J. Sham, "Self-consistent equations including exchange and correlation effects," Phys. Rev. **140**, A1133 (1965).

6. G. Kresse and J. Furthmuller, "Efficient iterative schemes for ab initio total-energy calculations using a plane-wave basis set," Phys. Rev. **B54**, 11169 (1996).
7. D. Vasileska D., S. M. Goodnick, and S. Goodnick, *Computational Electronics: Semiclassical and Quantum Device Modeling and Simulation* (CRC, 2010).
8. D. Yu. Protasov, T. V. Malin, A. V. Tikhonov, A. F. Tsatsul'nikov, and K. S. Zhuravlev, "Electron scattering in AlGaN/GaN heterostructures with a two-dimensional electron gas," Semiconductors, **47**, 33–44 (2013).
9. V. I. Zubkov, "Simulation of capacitance–voltage characteristics of heterostructures with quantum wells using a self-consistent solution of the Schrödinger and Poisson Equations," Semiconductors **40**, 1204–1208 (2006).
10. I. Supryadkina, K. Abgaryan, D. Bazhanov, and I. Mutigullin, "Study of the polarizations of (Al,Ga,AlGa)N nitride compounds and the charge density of various interfaces based on them," Semiconductors **47** (12), 1621–1625 (2013).
11. A. Trellakis, A. T. Galick, A. Pacelli, and U. Ravaioli, "Iteration scheme for solution of the two-dimensional Schrödinger–Poisson Equations in quantum structures," J. Appl. Phys. **81** (12) (1997).
12. A. Trellakis and U. Ravaioli, "Computational issues in the simulation of semiconductor quantum wires," Comput. Methods. Appl. Mech. Eng. **181**, 437–449 (2000).
13. A. Trellakis, A. T. Galick, A. Pacelli, and U. Ravaioli, "Comparison of iteration schemes for the solution of the multidimensional Schrodinger–Poisson Equations," VLSI Design **8** (1–4), 105–109 (1997).
14. C. Cohen-Tannoudji, B. Diu, and F. Laloë, *Mécanique quantique* (Hermann, Paris, 1977; URSS, Moscow, 2015).
15. R. P. Fedorenko, *Introduction to Computational Physics* (Intellekt, Moscow, 2008) [in Russian].
16. Z. Yarar, B. Ozdemir, and M. Ozdemir, "Mobility of electrons in a AIGaN/GaN QW: Effect of temperature, applied field, surface roughness and well width," Phys. Stat. Sol. (b) **242** (14), 2872–2884 (2005).

Translated by A. Klimontovich